A Two-stage Sensing Technique for Dynamic Spectrum Access

Ling Luo*, *Student Member*, Nathan M. Neihart†, *Member*, Sumit Roy*, *Fellow, IEEE* and David J. Allstot*, *Fellow, IEEE*
*Dept. of Electrical Engineering, Univ. of Washington, Seattle, WA, 98195, USA
†Now with Dept. of Electrical and Computer Engineering, Iowa State Univ., Ames, IA, 50011, USA

***Abstract*— Dynamic spectrum access (DSA) is a promising approach for the more effective use of existing spectrum. Of fundamental importance to DSA is the need for fast and reliable spectrum sensing over a wide bandwidth. A model for two-stage sensing is described based on an analysis of the mean time to detect an idle channel. Simulation results show that it provides significantly faster idle channel detection than conventional single-stage random searching. Several system-level issues are also investigated including the settling time of the phase-locked loop (PLL) in the frequency synthesizer, which determines the channel switching time. Effects of the bandwidth of the coarse sensing block and the integration duration of the energy detector are also presented.**

I. Introduction

Traditionally, radios are constrained to operate within a band of frequencies that has been set aside for their sole use by regulatory bodies (so-called licensed bands). But with many legacy technologies present, and with many new wireless standards on the horizon, the sub-10GHz spectrum is quickly becoming saturated. Several well-known studies of spectrum utilization, however, definitively show that licensed and allocated spectrum is used inefficiently [1], [2]; for example, more than 50% of broadcast television channels in the Seattle, Washington area are unused, constituting known 'white spaces' in the spectrum [3]. Dynamic spectrum access (DSA) has thus been proposed as a means to improve spectral efficiency by opening the spectrum for use by (new) secondary users on a non-interfering basis with primary users. This idea is gaining traction with regulatory bodies as well as evidenced by the recent ruling of the FCC to open up a 700 MHz band for use on a dynamic basis.

The two primary approaches to DSA are centralized and distributed. In a centralized spectrum sharing protocol [4], [5], a central coordinator (i.e., as a spectrum server) is responsible for coordinating the transmissions of a group of links sharing a common spectrum. By knowing the link gains in the network, the spectrum server organizes an optimal schedule that maximizes the average throughput of the network. In distributed systems [6], each transmitter/receiver pair must find an idle channel in which to communicate. Several studies have shown that varying levels of cooperation can increase the overall throughput of the network [7], [8].

One common requirement of both approaches is the fast and effective detection of idle primary channels by secondary users as characterized by the mean time for detection. The average time to successfully sense an available channel depends on the search algorithm, which can be broadly classified as either random (Fig. 1(a)), or deterministic (Fig. 1(b), bottom) [10], [11]. The performance of channel sensing is fundamental to many other sensing aspects for cognitive radios. The importance of detector design is further enhanced by the impact of its operating characteristic (represented by the probabilities of correct detection, P_d, and false alarm, P_{fa}, respectively) on the aggregate throughput when such a *DSA network* is operative [18].

Other than the sensing algorithm, system performance also depends on the sensing *architecture*; our work espouses a *two-stage* DSA approach (Fig. 1(b)) that comprises preliminary coarse resolution sensing (CRS) [11] followed by fine resolution sensing (FRS). The total spectrum is first partitioned into several contiguous coarse sensing blocks (CSB) of equal bandwidth; each is denoted as either CSBW with or CSBN without idle channels, respectively. FRS is then performed on a CSBW to detect an idle channel; if that process is unsuccessful, the search algorithm returns to the CRS stage. In this paper, analytical and simulation results for the mean detection time are developed for the two-stage DSA scheme. Trade-offs among the CSB bandwidth, integration duration, mean detection time and power dissipation are also explored.

II. System Description

A. System Model

Assume that the entire spectral band comprises an *N*-set of contiguous discrete frequency domain channels each with bandwidth, B_c, which also represents the bandwidth of a primary signal of interest. Let *L* be the number of idle channels (i.e., those unoccupied by primary users) where typically $L/N \ll 1$. Further, assume that the *L* idle channels are randomly scattered over the *N*-set. The binary variable, O_k, is used to denote the status of the k^{th} channel, where $O_k = 0(1)$ means the channel is busy (idle). Hence,

$$P(O_k = 1) = \frac{L}{N},\ k = 1, ..., N \tag{1}$$

This work was supported in part by the National Science Foundation under grant ITR/ANI 0325014 and by Semiconductor Research Corporation Contract 2006-HJ-1427, and a grant from the National Science Foundation Center for Design of Analog/Digital Integrated Circuits (CDADIC).

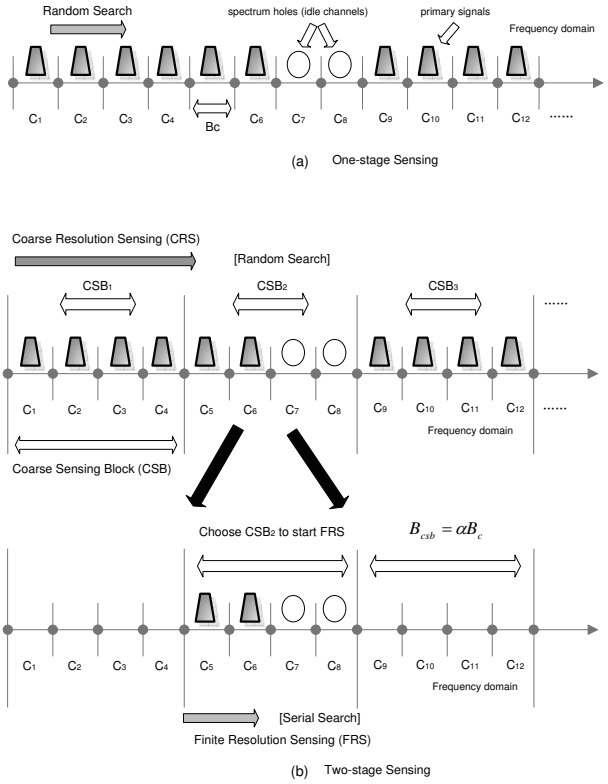

Fig. 1. Channel model and (a) one-stage (random search) and (b) two-stage (random and serial searches) sensing schemes.

All channels are assumed to be additive white Gaussian noise (AWGN) with normalized amplitude gains of unity. Moreover, the simplest and most widespread detection scheme is assumed; i.e., non-coherent energy detection wherein the observed signal samples are filtered to a detector bandwidth, B_{sense}, passed through a square-law detector, integrated over a sensing period, and compared to a decision threshold, D_t. P_n and P_{sig} are the noise and primary signal powers observed by the secondary user:

$$P_n = kTB_{sense} \quad (2)$$

$$P_{sig} = \overline{\gamma} P_n \quad (3)$$

where *k* is Boltzmann's constant (1.38×10^{23} J/°K), *T* is the system temperature (e.g., 300 °K), and $\overline{\gamma}$ is the average signal-to-noise ratio (*SNR*).

B. Channel Sensing

The conventional random search scheme is widely used in channel sensing. As illustrated in Fig. 1(a), if the secondary user randomly selects a channel that is detected to be busy, another channel is randomly chosen; the process repeats until an idle channel is found. In the serial search scheme, the secondary user searches sequentially beginning with an initial channel until an idle channel is discovered. Clearly, both random and serial searches are one-stage sensing schemes.

For $L/N \ll 1$, however, it has been shown that the detection performance of both one-stage schemes is inadequate because long mean times to detection are required [11]; hence, new approaches are needed. For example, nodes equipped with multiple antennas allow parallel (simultaneous) multi-resolution scanning of disjoint frequency bands to improve the mean time to detection [9]. In our work, we adapt the concept of simultaneous scanning with multiple antennas to nodes with a single antenna by using *multiple (two) stage* scanning to achieve similar improvments. Gezici presented a similar idea [29], but his objective is accurate estimation while our's is fast channel sensing. As shown in Fig. 1(b), the total spectrum is divided into β coarse sensing blocks, each with α channels of equal bandwidth B_c ($\alpha = N/\beta, B_{csb} = \alpha B_c$). As described earlier, the sensing algorithm comprises two stages: coarse resolution sensing followed by fine resolution sensing. In CRS, the first CSBW is located; thereafter, FRS attempts to detect an idle channel within it. A random search is used in CRS with a detection bandwidth equal to that of the CSB; i.e., $B_{sense} = B_{csb}$. Although both random and serial searches exhibit similar detection time performance [11], random search provides a better fairness to allocate a potential free channel, whether it is at the beginning or end of the channel sequence. In contrast, because random search can cause unnecessary death lock, FRS employs a serial search within a CSB with $B_{sense} = B_c$. This occurs if a false alarm in CRS occurs (i.e., the detector indicates an idle channel in the CSB when all are actually busy); a random search during the subsequent FRS would continue to try but fail to locate this nonexistent free channel – a death lock. However, the use of a serial search in FRS easily avoids the death lock because it evaluates all channels only once. If no idle channel is detected during FRS, the device returns to the CRS mode as illustrated in Fig. 2. If a false alarm (detecting a busy channel as idle) occurs during FRS, a penalty equal to *J* integration periods is incurred for recovery from the error before scanning is resumed.

III. Settling Time and Energy Consumption Trade-Offs

Inherent in the two-stage sensing algorithm is the need to quickly and efficiently jump from one channel frequency to another as the maximum frequency hop in either the CRS or FRS stage may span the entire frequency spectrum of interest. The settling time required for such frequency hopping is primarily determined by the design of the phase-locked loop (PLL) used in the frequency synthesizer that generates the channel carrier frequencies. It is well known that a conventional PLL designed with a wider bandwidth achieves a faster settling time. However, its phase noise is increased resulting in increased reciprocal mixing [27] and decreased *SNR* with a corresponding increase in detection errors. A decrease in settling time also comes at the expense of an increase in power dissipation with an attendant increase in the *energy cost* of spectrum sensing (i.e., Joules per Hz sensed). In this section, tradeoffs among settling time, phase noise and energy consumption in a PLL are described in the context of DSA applications.

Fig. 3 shows a block diagram of a typical type-II third-order PLL, which comprises five main components: the reference oscillator, the phase-frequency detector (PFD) and it

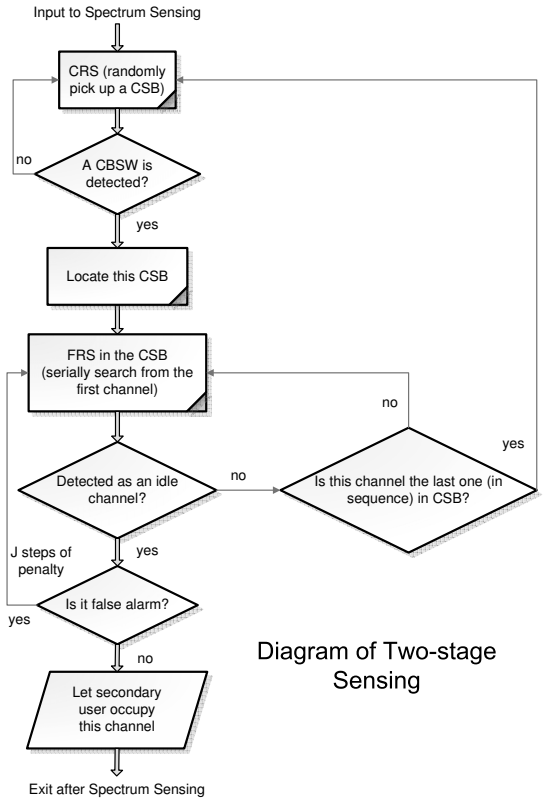

Fig. 2. Flow diagram for the two-stage sensing algorithm.

associated charge pump (CP), the low-pass loop filter (LPF), the voltage-controlled oscillator (VCO) and the feedback $\div N$ digital divider. The reference frequency, f_{ref}, is typically derived from a fixed low-frequency oscillator (e.g., a crystal oscillator). The PFD/CP combination produces a bi-directional current with magnitude proportional to the phase error, $\phi_e = \phi_{in} - \phi_{out}$. The output of the charge pump is filtered by the LPF to produce the VCO control voltage. The VCO, in turn, outputs a frequency, f_{out}, that is proportional to the control voltage. Owing to the negative feedback action of the PLL, the reference frequency is effectively multiplied by *N* to produce the desired channel carrier frequency. For a PLL that must generate the wide range of frequencies required for spectrum sensing in cognitive radios, the feedback digital divider ratio *N* is varied to select different channels with $f_{out} = N f_{ref}$.

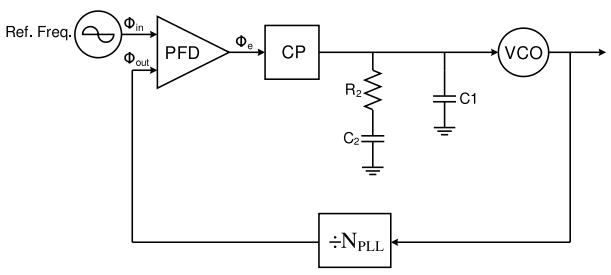

Fig. 3. Block diagram of a typical type-II, thrid-order PLL.

In two-stage sensing, the time available for the receiver to switch its sensing circuitry to a new channel is usually fixed. It is determined by the settling time of the PLL, which is the time needed for the control voltage of the VCO, or equivalently its output frequency, to settle within a predetermined accuracy of its final value, when the feedback divider value is switched to a new channel setting. Increased loop bandwidth in the PLL leads to faster settling and quicker detection of idle channels, but, for constant power dissipation, it trades off against increased phase noise. Consequently, power dissipation is often increased to reduce the phase noise spectral density [28].

A better understanding of the tradeoff between settling time and overall phase noise is gained by considering two components: phase noise contributed by (i) the reference oscillator, and (ii) the VCO. Phase noise contributed by the reference oscillator (i.e., reference noise) is filtered by the closed-loop transfer function of the PLL, *H(s)*, before it appears at the output. Hence, an increase in the closed-loop bandwidth to reduce settling time results in an increase in the total phase error integrated over that bandwidth [19], [20]. Conversely, VCO phase noise is shaped by the PLL closed-loop phase error transfer function, *E(s)*, given by

$$E(s) = 1 - H(s) \tag{4}$$

which has a high-pass characteristic. The PLL design tradeoffs are now clear: as the closed-loop bandwidth is increased, the settling time and low-frequency phase noise of the VCO are decreased, but the reference phase noise is increased. It can be shown that the phase noise contributions from the feedback digital divider and the PFD/CP are also high-pass shaped by *E(s)*. For simplicity, it is assumed in the following that the overall phase noise of the PLL is dominated by that of the reference.

As described above, fast settling time and low phase noise are achieved simultaneously by increased power dissipation. This tradeoff is validated in Table I, which compares five different PLL designs under the same phase noise constraints [21]-[25].

Although a conventional PLL cannot simultaneously achieve fast settling and low phase noise with low power dissipation, more sophisticated architectures overcome these tradeoffs. For example, in adaptive-loop architectures, the loop bandwidth of the PLL is increased, and thus the settling time is reduced, only during the frequency switching transient [26]. After the transient has subsided as indicated by the acquisition of phase lock, the loop bandwidth, and hence the corresponding phase noise, is reduced. This technique enables fast settling with low phase noise and low power dissipation and avoids the stability problems that plague conventional wideband phase-locked loops. Note that energy is consumed at a rate *E* per unit time during the entire integration period of the energy detector, $\overline{T}_{det}$; hence, the total energy cost is:

$$E_{total} = \overline{T}_{det} P \tag{5}$$

IV. Analysis of Detection and False Alarm Probabilities in Two-stage Sensing

A. Detection and False Alarm in FRS

During the fine resolution sensing stage, the sensing bandwidth of the energy detector is equal to the channel bandwidth; i.e., $B_{sense} = B_c$. The decision process chooses one of two hypotheses where H_1 and H_0 denote noise only and noise plus a primary signal, respectively. The output amplitude of an observed sample from the device, *x*, is represented by Gaussian probability density functions [11]

$$f(x|H_1) = \frac{1}{\sqrt{2\pi}\sigma_n}\exp\left(-\frac{x^2}{2\sigma_n^2}\right) \quad (6)$$

$$f(x|H_0) = \frac{1}{\sqrt{2\pi}\sigma_n}\exp\left(-\frac{(x-\sqrt{P_{sig}})^2}{2\sigma_n^2}\right) \quad (7)$$

where $\sigma_n = \sqrt{P_n/2} = \sqrt{kTB_c/2}$.

Let *z* denote the final decision variable after time integration; i.e., $z = \sum_{i=1}^{M_f} x_i^2$ where $M_f = \lfloor B_c \cdot T_i^f \rfloor$ ($\lfloor x \rfloor$ is the largest integer contained in x), and T_i^f is the integration time of the non-coherent detector used during FRS. It is clear that z follows a chi-square distribution under the null hypothesis, H_1, and a non-central chi-square distribution under H_0, both with M_f degrees of freedom [17]

$$f(z|H_1) = \frac{(1/2)^{M_f}}{\Gamma(M_f)} z^{M_f-1}e^{-z/2} \quad (8)$$

$$f(z|H_0) = \frac{1}{2}e^{-\frac{z+\lambda}{2}}(z/\lambda)^{\frac{M_f-1}{2}} I_{M_f-1}(\sqrt{z\lambda}) \quad (9)$$

where $\lambda = \sum_{i=1}^{M_f}\left(\frac{\mu_{xi|H_i}}{\sigma_{xi|H_i}}\right) = M_f\left(\frac{\sqrt{P_{sig}}}{\sqrt{P_n}}\right) = M_f\overline{\gamma}$, Γ is the gamma function defined by $\Gamma(z) = \int_0^\infty t^{z-1}e^{-t}dt$, and $I_{M_f}(x)$ is the first-order Bessel function $I_n(x) = \frac{x}{2}\left[1 - \frac{(x/2)^2}{2(1!)^2} + \frac{(x/2)^4}{3(2!)^2} - \frac{(x/2)^6}{4(3!)^2} + \ldots\right]$.

During the FRS stage the detection (P_d^f) and false alarm (P_{fa}^f) probabilities correspond to the successful detection by the secondary user of an idle channel under H_1 with no primary signal present under H_0. Hence, P_d^f and P_{fa}^f of the non-coherent detector in FRS are [15], [16]:

$$P_d^f = F_{z|H_1}(D_t/\sigma_n^2) = \frac{\overline{\gamma}(M_f, D_t/2\sigma_n^2)}{\Gamma(M_f)} \quad (10)$$

$$P_{fa}^f = F_{z|H_0}(D_t/\sigma_n^2) = 1 - Q_{M_f}\left(\sqrt{2\overline{\gamma}M_f}, \sqrt{D_t/\sigma_n^2}\right) \quad (11)$$

where $\overline{\gamma}$ is the lower incomplete gamma function, $\overline{\gamma}(a,x) = \int_0^x t^{a-1}e^{-t}dt$, and Q_m is the generalized Marcum Q-function $Q_M(\alpha,\beta) = \frac{1}{\alpha^{M-1}}\int_\beta^\infty x^M e^{-(x^2+\alpha^2)/2} I_{M-1}(\alpha x)dx$.

TABLE I
Measured Settling Time and Power Consumption of Five Different PLLs

Reference	Settling Time (T_s) [μs]	Power (P) [mW]
[21]	0.009	124
[22]	0.15	57.6
[23]	20	20
[24]	70	11.4
[25]	120	4.2

B. Detection and False Alarm in CRS

The analysis of the CRS sensing stage is more complex although the decision process again chooses between one of two hypotheses: H_1' when there exists at least one idle channel in the CSB and H_0' when there is none. If hypothesis H_1' is true, the FRS stage is invoked to identify an idle channel contained in the CSB. In the independent identically distributed (*i.i.d*) model, the *L* idle channels are randomly scattered over the *N*-set of channels and a primary signal occupies a specific channel with probability $(1-L/N)$. Therefore, the number of idle channels, *n*, in a coarse sense block follows a binomial distribution; i.e., $n \sim B(\alpha, L/N)$. As a sub-hypothesis of H_1', $H_{1(k)}'$ denotes the event that there are exactly *k* idle channels $(1 \le k \le \alpha)$ in a CSB assuming $\alpha \le L$; hence,

$$Pr(H_{1,(k)}') = Pr(n=k) = \binom{\alpha}{k}\left(\frac{L}{N}\right)^k\left(1-\frac{L}{N}\right)^{\alpha-k} \quad (12)$$

$$Pr(H_1') = 1 - Pr(n=0) = 1 - \left(\frac{N-L}{N}\right)^\alpha \quad (13)$$

$$Pr(H_{1,(k)}'|H_1') = \frac{Pr(n=k)}{Pr(H_1')} = \binom{\alpha}{k}\frac{L^k(N-L)^{\alpha-k}}{N^a - (N-L)^a} \quad (14)$$

The probability density functions of the measurements, *y*, that are inputs to the CRS detector, conditional on the two hypotheses, are thus given by

$$f(y|H_{1,(k)}') = \frac{1}{\sqrt{2\pi}\sigma_n'}\exp\left(-\frac{(x-(\alpha-k)\sqrt{P_{sig}})^2}{2{\sigma_n'}^2}\right) \quad (15)$$

$$f(y|H_0') = \frac{1}{\sqrt{2\pi}\sigma_n'}\exp\left(-\frac{(x-\alpha\sqrt{P_{sig}})^2}{2{\sigma_n'}^2}\right) \quad (16)$$

For the non-coherent detector during the coarse resolution stage, the noise power at the detector input is $\sigma_n' = \sqrt{P_n'/2} = \sqrt{\alpha P_n/2}$. Hence, the noise power is amplified by the factor α relative to that in the FRS scenario whereas the signal power remains the same.

Assuming the detector uses M_c samples, the decision statistic is $z = \sum_{i=1}^{M_c} y_i^2$ where $M_c = \lfloor B_{csb}T_i^c \rfloor$, and T_i^c is the integration time of the non-coherent detector used during CRS. Therefore, the detection, P_d^c, and false alarm, P_{fa}^c, probabilities are given by

$$P_d^c = F_{z|H_1'}(D_t'/{\sigma_n'}^2) = \sum_{k=1}^{\alpha} F_{z|H_{(k)}'}(D_t'/{\sigma_n'}^2)Pr(H_{(k)}'|H_1')$$

$$= \sum_{k=1}^{\alpha} Pr(H_{1,(k)}'|H_1')\left[1 - Q_{M_c}\left(\sqrt{2\frac{\alpha-k}{\alpha}\overline{\gamma}M_c}, \sqrt{\frac{D_t'}{\alpha\sigma_n^2}}\right)\right] \quad (17)$$

$$P_{fa}^c = F_{z|H_0'}(D_t'/{\sigma_n'}^2) = 1 - Q_{M_c}\left(\sqrt{2\overline{\gamma}M_c}, \sqrt{D_t'/\alpha\sigma_n^2}\right) \quad (18)$$

In most practical cases, the number of available channels is no less than the number of channels in a CSB ($\alpha \le L$). However, there might be just few a available channels through the whole spectrum, causing $L < \alpha$; hence, in this extreme

case,

$$Pr(H_1') = \sum_{i=1}^{L} Pr(H'_{1,(i)}) = \sum_{i=1}^{L} \binom{\alpha}{i} \left(\frac{L}{N}\right)^i \left(1-\frac{L}{N}\right)^{\alpha-i} \quad (19)$$

$$Pr(H'_{1,(k)}|H_1') = \frac{Pr(n=k)}{Pr(H_1')} = \binom{\alpha}{k} \left(\frac{L}{N}\right)^k \left(1-\frac{L}{N}\right)^{\alpha-k} / Pr(H_1') \quad (20)$$

$$P'_{cd} = \sum_{k=1}^{L} Pr(H'_{1,(k)}|H_1') \left[1 - Q_{M_c}\left(\sqrt{2\frac{\alpha-k}{\alpha}}\gamma M_c, \sqrt{\frac{D'_t}{2}}\right)\right] \quad (21)$$

V. Mean Detection Time

Each channel scanning period comprises two subintervals: T_s and T_i. T_s is the settling time of the PLL used in the frequency synthesizer, which depends on its type and order as well as other circuit details. T_i is the integration time required for the non-coherent detector to reach a decision on the status of the channel (i.e., busy or idle); it is a function of the detector configuration and the desired value of $P_d - P_{fa}$, which is a measure of accuracy.

The overall mean detection time, $\overline{T}_{det}$, required for a secondary user to successfully identify an idle channel is a function of the two subintervals mentioned above; i.e.,

$$\overline{T}_{det} = \overline{S}_{det}(T_s + T_i) \quad (22)$$

where $\overline{S}_{det}$ is the average number of steps required for acquisition.

The mean number of detection steps required for conventional random and serial searches is derived by Luo, et al. [11]:

$$\overline{S}_{ran} = \frac{(N-L)J * P_{fa}^f + N}{P_d^f L} = \frac{(1-\frac{L}{N})J * P_{fa}^f + 1}{P_d^f \frac{L}{N}} \quad (23)$$

$$\overline{S}_{ser} = \frac{(N-L)J * P_{fa}^f + N}{P_d^f (L+1)} \quad (24)$$

In the ideal scenario where $P_d = 1$ and $P_{fa} = 0$, (23) and (24) simplify to

$$\overline{S}_{ran,ideal} = \frac{N}{L} \quad (25)$$

$$\overline{S}_{ser,ideal} = \frac{N}{(L+1)} \quad (26)$$

The average number of detection steps required for two-stage sensing is determined next.

A. Analysis of Two-Stage Sensing

The mean number of total detection steps in the coarse plus fine resolution stages is

$$\overline{S}_{det} = \overline{S}_{crs} + \overline{S}_{frs} \quad (27)$$

In the i.i.d model, each CSB has the same probability, $P_r(H_1')$, of containing a white space. Hence, similar to the analysis of the conventional random search, the mean number of steps required during the CRS stage to successfully detect an idle channel in a coarse sensing block is

$$\overline{S}_{crs,det} = \frac{1}{Pr(H_1')P_d^c} \quad (28)$$

However, if no idle channels are found during an FRS stage, the CRS stage is re-initialized, which occurs with probability $a=i$

$$P_{miss} = \sum_{k=1}^{\alpha} Pr(H'_{(k)}|H_1')(1-P_d^f)^k \quad (29)$$

$$= \sum_{k=1}^{\alpha} \binom{\alpha}{k} \frac{L^k(N-L)^{\alpha-k}}{N^a-(N-L)^a}(1-P_d^f)^k$$

The number of steps for such missed detection follows a geometric distribution with an expected value of $1/(1-P_{miss})$. Thus, the average total number of steps during the CRS stage is given by

$$\overline{S}_{crs} = \overline{S}_{crs,det}/(1-P_{miss}) = \frac{1/[(1-(\frac{N-L}{N})^\alpha)P_d^c]}{1-\sum_{k=1}^{\alpha}\binom{\alpha}{k}\frac{L^k(N-L)^{\alpha-k}}{N^a-(N-L)^a}(1-P_d^f)^k} \quad (30)$$

The analysis of the FRS stage is divided into two conditional events: (a) after correct detection, and (b) after false alarm in the CRS stage to yield $\overline{S}_{frs,cor}$ and $\overline{S}_{frs,fal}$, respectively. Assuming that exactly i idle channels exist in a CSB (i.e., $n=i$), the mean number of steps required by FRS is given by [11]

$$\overline{S}_{frs,cor} = E[S_{frs,cor}|n=i] = \sum_{i=1}^{\alpha}\binom{\alpha}{i}\frac{L^i(N-L)^{\alpha-i}}{N^a-(N-L)^a}\frac{(\alpha-i)J*P$$
$$P_d^f \cdot$$

(31)

For each false alarm during a CRS stage, the subsequent FRS stage uses $\alpha(1+JP_{fa}^f)$ more steps on average before discovery. Because the probability of a CSB with at least one idle channel is $Pr(H_1')$, the mean number of steps caused by false alarm in CRS is

$$\overline{S}_{frs,fal} = (1-Pr(H_1'))P_{fa}^c\overline{S}_{crs,det}(1+J*P_{fa}^f)\alpha = \frac{P_{fa}^c\alpha(1+J*P_{fa}^f)(N-L)^k}{P_d^c(N^k-(N-L)^k)} \quad (32)$$

Hence, the expected number of steps for FRS sensing, $\overline{S}_{frs}$, is given by

$$\overline{S_{frs}} = (\overline{S_{frs,cor}}+\overline{S_{frs,fal}})/(1-P_{miss}) = \frac{\sum_{i=1}^{\alpha}\binom{\alpha}{i}\frac{L^i(N-L)^{\alpha-i}}{N^a-(N-L)^a}\frac{(\alpha-}{}}{1-\sum_{k=1}^{\alpha}\binom{\alpha}{k}}$$

(33)

In the ideal scenario with $P_d^f = P_d^c = 1$ and $P_{fa}^f = P_{fa}^c = 0$, the overall mean number of detection steps simplifies to

$$\overline{S}_{det} = \sum_{i=1}^{\alpha}\binom{\alpha}{i}\frac{L^i(N-L)^{\alpha-i}}{N^a-(N-L)^a}\cdot\frac{\alpha}{i} + \frac{1}{1-(\frac{N-L}{N})^\alpha} \quad (34)$$

B. Overall Mean Detection Time

At each sensing stage, an increased number of samples (pre-detection integration) results in a more reliable outcome as determined by higher detection and lower false alarm probabilities, which in turn leads to fewer steps required on average for detecting an available idle channel. Let M_c and M_f denote the number of sensing samples in the CRS and FRS

stages, respectively. Then the corresponding mean detection time ($\overline{T}_{det}$) is expressed in terms of T_i^c and T_i^f, the integration periods for CRS and FRS, respectively:

$$\overline{T_{det}} = \overline{S_{frs}}(T_s + T_i^f) + \overline{S_{crs}}(T_s + T_i^c) \quad (35)$$

where

$$T_i^c = \frac{M_c}{\alpha B_c} \quad (36)$$

$$T_i^f = \frac{M_f}{B_c} \quad (37)$$

Upon substitution, (35)-(37) can be re-written in the final form as

$$\overline{T_{det}} = \frac{\sum_{i=1}^{\alpha}\binom{\alpha}{i}\frac{L^i(N-L)^{\alpha-i}}{N^a-(N-L)^a}\frac{(\alpha-i)J*P_{fa}^f+\alpha}{P_d^f\cdot i} + \frac{P_{fa}^c\alpha(1+J*P_{fa}^f)2(N-L)^k}{P_d^c(N^k-(N-L)^k)}}{[1-\sum_{k=1}^{\alpha}\binom{\alpha}{k}\frac{L^k(N-L)^{\alpha-k}}{N^a-(N-L)^a}(1-P_d^f)^k]/(T_s+\frac{M_f}{B_{min}})} + \frac{(T_s+\frac{M_c}{\alpha B_{min}})/[(1-(\frac{N-L}{N})^\alpha)P_d^c]}{1-\sum_{k=1}^{\alpha}\binom{\alpha}{k}\frac{L^k(N-L)^{\alpha-k}}{N^a-(N-L)^a}(1-P_d^f)^k} \quad (38)$$

Intuitively, shorter PLL settling time leads to shorter mean detection time. However, the power dissipation per unit time is also increased in order to maintain the same phase noise level. Since the total energy cost is composed of energy in the PLL settling stage plus energy in the energy detector stage, it is also interesting to investigate the trade-off between detection time and total energy consumption. Such results are given in the next Section.

C. Overall $P_d - P_{fa}$

In two-stage sensing, the overall accuracy of the system (i.e., $(P_d - P_{fa})$) depends on the decision thresholds for the two stages:

$$P_d = P_d^c P_d^f \quad (39)$$

$$P_{fa} = 1 - (1 - P_{fa}^c)(1 - P_{fa}^f) \quad (40)$$

The FRS stage has the same receiver operating characteristics (ROC) as in one-stage sensing, because both operate under the same conditions using the same approach. The ROC is shown in Fig. 4 for several values of M_f.

To gain additional insight into the operation of the two-stage sensing scheme, the ROC is held constant during the FRS stage ($P_d^f = 0.9, M_f = 4$, and $\overline{\gamma} = 6dB$ (the per sample *SNR* at the front-end of the detector)), while the parameters of the CRS stage are varied to determine the effects on the overall $(P_d - P_{fa})$. Figs. 5 and 6 plot the P_m vs. P_{fa} performances ($P_m = (1 - P_d)$) of the non-coherent energy detector for different values of M_c, α and L/N. It is observed that a wider CSB bandwidth results in decreased $(P_{fa} - P_m)$ performance due to the increased noise power. Although $(P_{fa} - P_m)$ performance always improves by integrating over more sensing samples, a significantly larger number were required to achieve the desired $(P_{fa} - P_m)$ performance. Moreover, the performance of the system benefits from the smaller values of P_m associated with the larger values of L/N.

In a typical TV spectrum, the total system bandwidth is B_{sys} = 1.2 GHz and the channel bandwidth is B_c = 6 MHz; hence, the number of channels is $N = B_{sys}/B_c = 200$. Considering different average values of *SNR* ($\overline{\gamma}$) at the input to the non-coherent detector, the integration durations needed during the CRS stage to achieve $P_d^f = 0.9, P_{fa}^f = 0.05, P_d^c = 0.8$, and $P_{fa}^c = 0.15$ are given in Table II.

TABLE II
CRS INTEGRATION PERIODS FOR P_d^f = 0.9, P_{fa}^f = 0.05, P_d^c = 0.8 AND P_{fa}^c = 0.15

		L/N = 0.1		*L/N = 0.2*		*L/N = 0.3*	
α	$\overline{\gamma}$(dB)	M_c	$T_i^c(\mu s)$	M_c	$T_i^c(\mu s)$	M_c	$T_i^c(\mu s)$
2	3	25	2.1	25	2.1	24	2
4	3	110	4.6	100	4.2	90	3.8
10	3	600	10	370	6.2	170	2.8
2	6	11	0.9	11	0.9	10	0.8
4	6	50	2.1	44	1.8	38	1.6
10	6	270	4.5	160	2.7	70	1.2
2	13	2	0.17	2	0.17	2	0.17
4	13	8	0.33	7	0.29	6	0.25
10	13	40	0.67	24	0.4	12	0.2

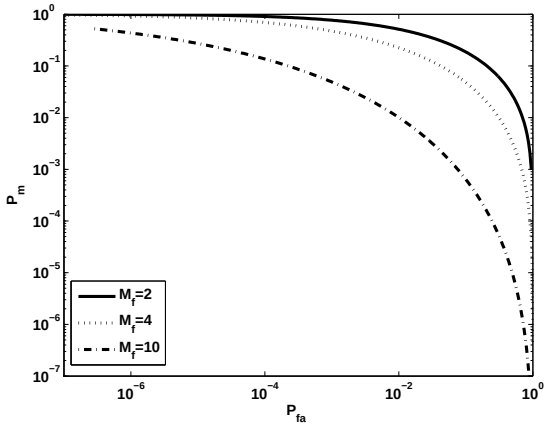

Fig. 4. Receiver operating characteristics for one-stage sensing FRS with SNR = 6 dB.

VI. NUMERICAL RESULTS

In this section, experimental results are used to compare the performance of the conventional one-stage (random search) and proposed two-stage (random then serial searches) sensing schemes; the simulations assume T_s is 0.15 μs, 20 μs and 120 μs for type-I [22], type-II [23] and type-III [25] PLL designs, respectively. *MATLAB* is used to generate the discrete channel frequencies, and the data is gathered after running 3000 realizations for each experiment. For convenience, the numerical results are separated according to the *SNR* values at the front-end of the detector; i.e., case I: $\overline{\gamma}$ = 3 dB; case II: $\overline{\gamma}$ = 6 dB and case III: $\overline{\gamma}$ = 13 dB. These three cases correspond to low-, mid-, and high-SNR environments, respectively. An SNR greater than 13dB is practical but leads to similar mean detection time results as for case III because the sensing duration is small relative to the settling time, especially for type-I and type-II PLL designs.

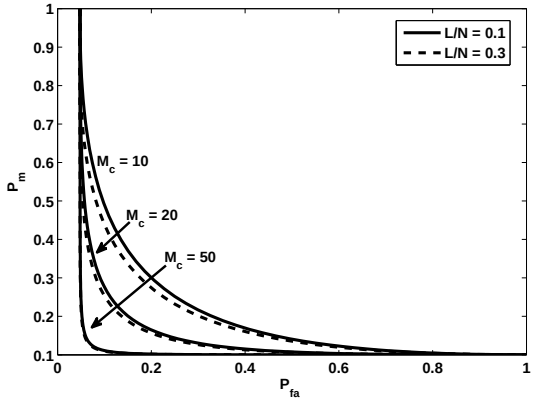

Fig. 5. Overall receiver operating characteristics of two-stage sensing with SNR = 6 dB, $M_f = 4$, $\alpha = 2$, and $Pf_d = 0.9$.

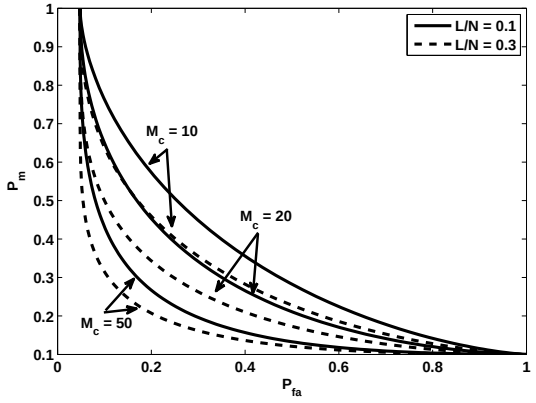

Fig. 6. Overall receiver operating characteristics of two-stage sensing with SNR = 6 dB, $M_f = 4$, $\alpha = 4$, and $Pf_d = 0.9$.

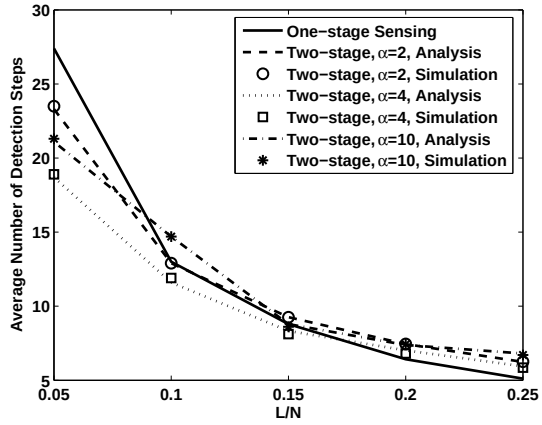

Fig. 7. Average number of detection steps for the one- and two-stage sensing schemes versus L/N and the CSB bandwidth.

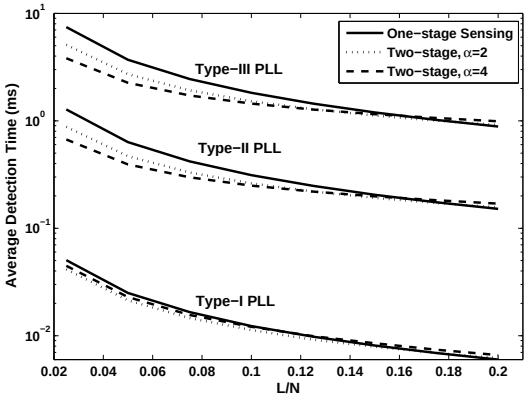

Fig. 8. Average detection time: case I.

A. Mean Detection Time

The average numbers of detection steps required for the conventional one-stage and proposed two-stage sensing schemes are first compared with P_d^f = 0.9, P_{fa}^f = 0.05, P_d^c = 0.8 and P_{fa}^c = 0.15, and *J* = 4. As demonstrated in Fig. 7 with α = 2, 4 and 10 (i.e., B_{csb} = 12, 24 and 60 MHz), the analytical formulations presented above are in good agreement with the simulation results. The results show that the two-stage sensing is generally preferable, especially when L/N is small. However, the mean number of detection steps required for one-stage sensing decreases dramatically as L/N increases, and eventually becomes slightly smaller than that of the two-stage scheme due to the increased mean number of steps required in the CRS stage. Fig. 7 also illustrates a weakness of multiple-stage sensing: overall efficiency is reduced because of needless transfers between stages due to missed detects or false alarms in the fine resolution stage(s).

The bandwidth of the CSB introduces another trade-off; i.e., a small bandwidth means a large number of detection steps to locate a CSBW whereas a large bandwidth costs more time in the FRS stage. To further explore this trade-off, the average detection time is simulated for different values of CSB bandwidth, L/N, $\overline{\gamma}$ and types of PLL circuits used in the frequency synthesizers. In Fig. 8, two-stage sensing with α = 2 and 4 outperforms one-stage sensing for $L/N < 0.15$ for all PLL types; the advantage is most significant in medium and high *SNR* environments. For $L/N < 0.1$ for a type-I PLL, two-stage sensing with α = 2 finds an idle channel faster than both the one-stage and two-stage with α = 4. In Fig. 9, two-stage sensing with α = 4 performs better than with α = 2 for both type-II and type-III PLLs. Fig. 10 shows similar results for all PLL types because the differences in integration durations for different CSB values in high-*SNR* environments is not as significant as in the low-*SNR* counterparts. The average detection time is sensitive to the product of the PLL settling time and the mean number of detection steps. For the same L/N, increasing the CSB bandwidth means more sensing samples, and an increased mean detection time, are needed to achieve the same performance in $P_d^c - P_{fa}^c$. However, two-stage sensing with $L/N < 0.15$ provides the best results for both type-II and type-III PLLs, which exhibit longer settling times than type-I designs in these examples, because of the smaller average number of detection steps associated with α = 4.

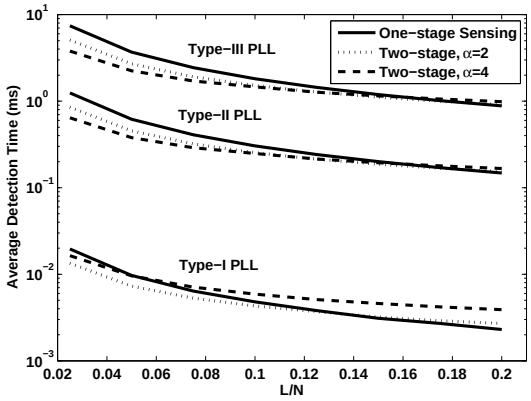

Fig. 9. Average detection time: case II.

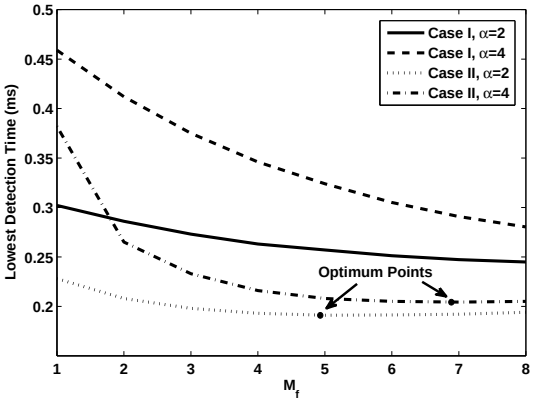

Fig. 11. The lowest detection time for different values of M_f.

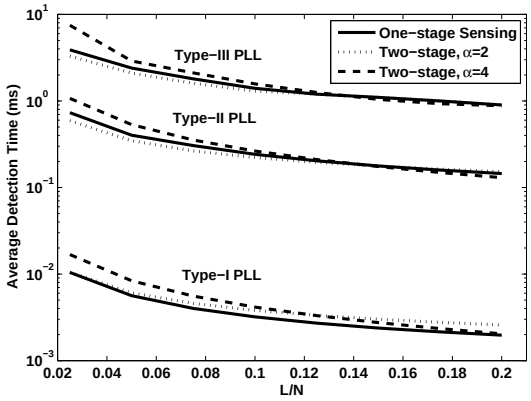

Fig. 10. Average detection time: case III.

B. Trade-Offs Between the CRS and FRS Stages

Fixing a maximum net integration time for the two-stage detection system imposes a trade-off between the CRS and FRS evaluation times. For example, an increase in the number of samples used in CRS yields better $(P_d^c - P_{fa}^c)$ performance but worse $(P_d^f - P_{fa}^f)$, and vice-versa. Based on this observation, there might be an optimum $(P_d^c/P_{fa}^c - P_d^f/P_{fa}^f)$ versus M_f (and M_c) that achieves that minimum detection time. This trade-off is illustrated in Fig. 11 for different values of $\overline{\gamma}$ and α for a type-II PLL with P_d^f = 0.9, L/N = 0.1, and $T_i = T_i^f + T_i^c = 5\ \mu s$. M_f = 5 is optimum for $T_i^f = 0.83\ \mu s$ and α = 2 (top) or M_f = 7 for T_i^f = 1.67 μs and α = 4. For case I, however, the detection time decreases monotonically with M_f because the allotted net integration time is insufficient. In a low-*SNR* environment, such a small integration time leads to a smaller range of $(P_d^f - P_{fa}^f)$ values than in a high-*SNR* situation. Hence, as described above, the system requires a large net integration time to possess an optimum value of M_f. For Fig. 11, for example, optimum M_f values exist for $T_i > 10\ \mu s$.

C. Trade-Offs Between Detection Time and Energy Consumption

Another critical trade-off in PLL design exists as a result of the burgeoning demand for low-energy systems: settling time versus energy consumption. For a given PLL type, the energy consumed due to circuit switching is $E_s = PT_s\overline{S}_{det}$. It comprises, along with that used during integration, the total energy consumption, $E_{total} = E_s + E_i$, where $E_i = PT_i$ and T_i is the integration period. It is shown in Fig. 12 for the examples used herein, that type-I PLL circuits exhibit the lowest energy consumption. Moreover, as the integration duration is relatively small for applications using the TV bands, E_i is a minor component of the total energy consumption. The relationship between power dissipation and settling time in a PLL is inherently nonlinear. Hence, the type-I PLL, which has the lowest value of PT_s, provides the minimum overall energy consumption in the TV-band dynamic sensing application.

For any of the PLL circuits used herein, one-stage sensing performs slightly better in terms of detection time for high L/N values. However, the situation is more complex for low L/N values. As shown in Fig. 12, the two-stage sensing with α = 10 performs better with a type-III PLL (T_s = 120 μs) but worse with type-I PLL (T_s = 0.15 μs), compared to the one-stage sensing. The two-stage sensing consumes more energy during integration, but this becomes less important as the PLL settling time increases. Compared with one-stage sensing, the two-stage sensing with α = 4 and 10 consumes less energy for settling times $>$ 0.15 μs, but more when the settling time is 0.009 μs.

VII. Conclusions

A two-stage sensing technique for Dynamic Spectrum Access for enhanced channel sensing in TV-band applications is described in this paper. This novel technique is investigated in terms of both detection theory and practical circuit constraints. The results show that two-stage sensing with a small bandwidth coarse sensing block outperforms the traditional one-stage sensing scheme in terms of lower mean detection time when the ratio of idle channels is low. System performance studies involving the bandwidth of the coarse sensing block

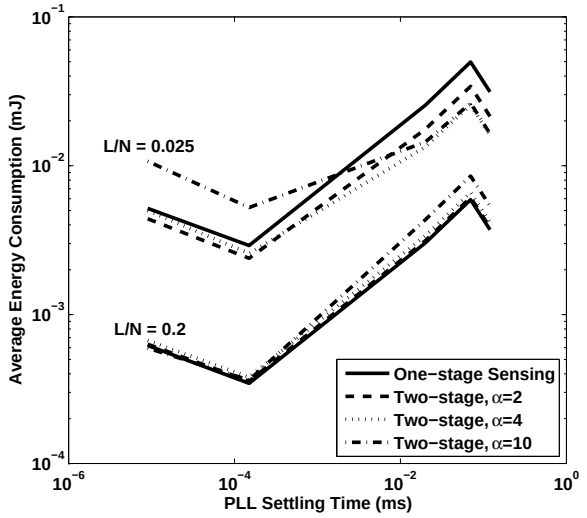

Fig. 12. Total energy consumption in case I with SNR = 3 dB.

also highlight the role of the integration time in both stages and the total energy cost in determining optimum designs.

REFERENCES

[1] FCC, *Spectrum Policy Task Force Report*, ET Docket No. 02-155, Nov. 2002.

[2] M. Nekovee, "Dynamic spectrum access - concepts and future architectures," *BT Technology Journal*, vol. 24, pp. 111-116, Apr. 2006.

[3] www.freepress.net/spectrum/whitespace/Seattle.pdf

[4] C. Raman, R. Yates, and N. Mandayam, "Scheduling variable rate links via a spectrum server," *Proc. of the first IEEE Sym. on New Frontiers in Dynamic Spectrum Access Networks*, pp. 110-118, 2005.

[5] O. Ileri, D. Samardzija, and N. Mandayam, "Demand responsive pricing and competitive spectrum allocation via a spectrum server," *Proc. of the first IEEE Sym. on New Frontiers in Dynamic Spectrum Access Networks*, pp. 194-202, 2005.

[6] R. Etkin, A. Parekh, and D. Tse, "Spectrum sharing for unlicensed bands," *Proc. of the first IEEE Sym. on New Frontiers in Dynamic Spectrum Access Networks*, pp. 251-258, 2005.

[7] S. Chung, S. Kim, J. Lee, and J. Cioffi, "A game-theoretic approach to power allocation in frequency-selective Gaussian interference channels," *Proc. IEEE Sym. on Information Theory*, pp. 316, June 2003.

[8] J. Huang, R. Berry, and M. Honig, "Spectrum sharing with distributed interference compensation," *Proc. of the first IEEE Sym. on New Frontiers in Dynamic Spectrum Access Networks*, pp. 88-93, 2005.

[9] N. M. Neihart, S. Roy and D. J. Allstot, "A parallel, multi-resolution sensing technique for multiple antenna cognitive radios," *IEEE Int. Symp. on Circuits and Systems*, pp. 2530-2533, May 2007.

[10] I Ramachandran and S. Roy, "On acquisition of wideband direct-sequence spread spectrum signals," *IEEE. Trans. on Wireless Commun.*, vol. 5, pp. 1537-1546, June 2006.

[11] L. Luo and S. Roy, "A two-stage sensing technique for dynamic spectrum access," *IEEE Int. Conf. on Communications*, pp. 4181-4185, May 2008.

[12] H. Kim and K. G. Shin, "Adaptive MAC-layer sensing of spectrum availability in cognitive radio networks," *Technical Report*, CSE-TR-518-06, University of Michigan, 2006.

[13] G. Ganesan and Y. Li, "Cooperative spectrum sensing in cognitive radio networks," *IEEE Int. Symp. on New Frontiers in Dynamic Spectrum Access Networks*, pp. 137-143, Nov. 2005.

[14] C. Cordeiro, K. Challapali and M. Ghosh, " ," *IEEE Int. Workshop on Technology and Policy for Accessing Spectrum*, No. 3, 2006.

[15] R. M. McDonough and A. D. Whalen, *Detection of Signals in Noise*, San Diego, CA: Academic Press, 1995.

[16] M. Abramowitz and I. A. Stegun, *Handbook of Mathematical Functions*, Dover. Section 26.4.25, 1972.

[17] H. Urkowitz, "Energy detection of unknown deterministic signals," *Proc. IEEE*, vol. 55, pp. 523-531, Apr. 1967.

[18] I. Ramachandran and S. Roy, "Clear channel assessment in energy constrained wideband wireless networks," *IEEE Wireless Commun. Magazine*, pp. 70-78, June 2007.

[19] F. M. Gardner, "Charge-pump phase-lock loops," *IEEE Trans. on Communications*, vol. 28, pp. 1849-1858, Nov. 1980.

[20] S. I. Ahmed and R. D. Mason, "Improving the acquisition time of a PLL-based, integer-N frequency synthesizer," *IEEE Int. Symp. on Circuits and Systems*, pp. 365-368, May 2004.

[21] R. van de Beek, D. Leenaerts, and G. van der Weide, "A fast-hopping single-PLL 3-band UWB synthesizer in 0.25μm SiGe BiCMOS," *European Solid-State Circuits Conf.*, pp. 173-176, Sept. 2005.

[22] Y. Tang, Y. Zhou, S. Bibykl, and M. Ismail, "A low-noise fast-settling PLL with extended loop bandwidth enhancement by new adaptation technique," *IEEE ASIC/SOC Conf.*, pp. 93-97, Sept. 2001.

[23] A. Ravi, R. E. Bishop, L. R. Carley, K. Soumyanath, "8GHz, 20mW, fast locking, fractional-N frequency synthesizer with optimized 3^{rd} order, 3/5-bit IIR and 3^{rd} order 3-bit-FIR noise shapers in 90nm CMOS," *IEEE Custom Integrated Circuits Conf.*, pp. 625-628, Oct. 2004.

[24] M. Marletta, P. Aliberti, M. Pulvirenti, A. Cavallaro, S. Terryn, P. Filoramo, R. Iardino, V. Spalma, and S. Cosentino, "Fully integrated fractional PLL for bluetooth application," *IEEE Radio Frequency IC Symp.*, pp. 557-560, June 2005.

[25] S. Shin, K. Lee, and S. M. Kang, "4.2mW CMOS frequency synthesizer for 2.4GHz ZigBee application with fast settling time performance," *IEEE Int. Microwave Theory and Tech. Symp.*, pp. 411-414, 2006.

[26] C.S. Vaucher, "An adaptive PLL turning system architecture combining high spectral purity and fast settling time," *IEEE J. Solid-State Circuits*, vol. 35, pp. 490-502, Apr. 2000.

[27] B. Razavi, "A study of phase noise in CMOS oscillators," *IEEE J. Solid-State Circuits*, vol. 31, pp. 331-343, March 1996.

[28] D. B. Leeson, "A simple model of feedback oscillator noise spectrum," *Proc. IEEE*, vol. 54, pp. 329-330, Feb. 1966.

[29] S. Gezici, Z Sahinoglu, A. F. Molisch, H. Kobayashi, and H. V. Poor, "A two-step time of arrival estimation for impulse pulse-based ultra-wideband systems," *EURASIP J. on Advances in Signal Processing*, vol. 2008, Article ID 529134, 2008.